

UCSF

UC San Francisco Electronic Theses and Dissertations

Title

Hierarchical Characterization and Correlation of Mineral Densities of Pathological Biominerals

Permalink

<https://escholarship.org/uc/item/8qx9w42g>

Author

Ellenikiotis, Yianni

Publication Date

2020

Peer reviewed|Thesis/dissertation

Hierarchical Characterization and Correlation of Mineral Densities of Pathological
Biominerals

by
Yianni Ellenikiotis

THESIS
Submitted in partial satisfaction of the requirements for degree of
MASTER OF SCIENCE

in
Oral and Craniofacial Sciences

in the
GRADUATE DIVISION
of the
UNIVERSITY OF CALIFORNIA, SAN FRANCISCO

Approved:

DocuSigned by:
Sunita Ho Sunita Ho
B3DEF15BD3D8415... Chair

DocuSigned by:
Sunil Kapila Sunil Kapila

DocuSigned by:
Andrew H. Jheon Andrew H. Jheon
F365EA7416024CA...

Committee Members

Acknowledgements

I would like to thank my thesis chair, Dr. Sunita Ho, and the entire team in Dr. Ho's lab that has helped contribute to the research behind this thesis. I would like to especially thank Dr. Sunita Ho, Misun Kang, and Sudarshan Srirangapatanam for the consistent collaboration and work throughout this process. Thanks to Merissa Ferrar, Todd Wedeking, Marshall Stoller, Youngho Seo, Dr. Sunil Kapila, and Dr. Andrew Jheon as well for your contributions and support.

Abstract

Hierarchical Characterization and Correlation of Mineral Densities of Pathological Biomaterials

Yianni Ellenikiotis

Cone beam computed tomography (CBCT) usage has increased dramatically over the last couple of decades. The extent to which this tool can be accurately utilized, however, remains to be seen. The purpose of this investigation is to produce a systematic, reproducible calibration of structure and mineral density, from micro X-ray computed tomography (Micro XCT) to CBCT. Three scanners were calibrated to known mineral density phantoms. Calibration curves for each scanner were built from these phantoms and hydroxyapatite specimens, which were then applied to determine the mineral density of human jaws and teeth. Systematic calibration accounting for size of the phantom (ratio of surface area to volume), and mineral density (the amount of mineral in “mg” per cubic centimeter volume “cc”) revealed that each scanner has a size and density dependence and thereby threshold limits for detectable size and mineral density of a specimen. Inferior resolution, large field of view, lower mineral density, and small size of specimens all contributed to reduced accuracy and consistency of CBCT images. Based on the current calibration and quality of CBCT systems, this research has shown that the accuracy of these scanners needs improvement and that screening for prevention of disease is likely beyond the current scope of its intended use. It is likely that a lesion or pathology can only be diagnosed reliably when it is of a large enough density and size to be imaged under a smaller field of view with enhanced resolution. Research is warranted to develop and implement protocols that would reliably use CBCT imaging as an effective screening tool to improve patient care.

Table of Contents

Introduction	1
CBCT versus panoramic X-rays	2
Imaging in orthodontics	5
Current and potential applications	6
Radiography, tomography and clinical scenarios	8
Bone mineral density measurements	11
Micro X-ray computed tomography	13
Calibration of scanners for quantitative measures of mineral density	14
Hypothesis	14
Materials and Methods	15
Computed tomography (CT) systems	15
Calibration of three CT systems	16
Specimens and comparisons of MDs	17
Size and shape effects of mineral density	19
Results	19
Discussion	32
References	39

List of Figures

Figure 1 Large and small phantoms	17
Figure 2 Calibration of computed tomography (CT), CBCT 1, CBCT 2 and Micro X-ray CT (Micro XCT)	20
Figure 3 Phantom Gray Value distributions and plot profiles of MD layers of 0, 100, 250, 500, and 750 mg/cc using different CT systems	21
Figure 4 Comparison of mineral densities between CBCT 1, CBCT 2 and Micro X-ray CT	24
Figure 5 MD differences of canines of patients using CBCT 1	26
Figure 6 Analysis of structures and materials of different CBCT 1 Images	28
Figure 7 Size and mineral density dependent signals as seen by CBCT and Micro XCT systems	30
Figure 8 Size dependent signal of hydroxyapatite (HA) calibration specimen	31

List of Tables

Table 1

Scanning parameters of computed tomography (CT) systems

15

List of Abbreviations

CBCT	Cone Beam Computed Tomography
CT	Computed Tomography
HA	Hydroxyapatite
HU	Hounsfield Unit
MD	Mineral Density
SA	Surface Area
SE	Standard Error
TMJ	Temporomandibular Joint
3D	Three-dimensional
2D	Two-dimensional
V	Volume

Introduction

X-ray computed tomography (CT) technology has rapidly transformed the field of healthcare. Traditionally, X-ray images have been two-dimensional (2D) which are useful in clinical diagnoses as they help formulate clinical plans. However, several limitations, including the ability to delineate pathophysiologic progression exist. Over the last few decades, CT's three-dimensional (3D) imaging capability has seen rapid technological progress. CT technology has allowed scientists and physicians to visualize internal structures and undoubtedly enhanced our diagnostic capabilities. 3D imaging also has dramatically increased radiation exposure to our patients, especially with repeated scans. As the technologies of CT scans steadily improved with greater mechanical stability, high throughput, and reduced radiation dose, CT has become more of a mainstream imaging system for emergency room visits and for specialized physicians and scientists. It is a central diagnostic and research tool of modern medicine and hints on its extension as a screening tool.

The current CT systems mostly use fanbeam and multi-detector images. Cone-beam CT (CBCT) is similar to these CT systems although it has wider collimation which can increase scatter radiation and worsen image quality. CBCT captures various distinct images of the patient by emitting energy through a beam like tube. As the tube rotates around the patient's region of interest for up to 20 seconds, it utilizes hundreds of projections to generate a 3D digital image. CBCT has many applications in both medical and dental fields – from orthopedics, interventional radiology, and image-guided radiation therapy to endodontics, implantology, oral surgery, and orthodontics. Dental CBCT is consistently used in various subspecialties of dentistry as it can reveal the

entire tooth including its roots within the jaws, surrounding structures, and condyles within the craniofacial complex.

CBCT versus panoramic X-rays

CBCT provides windows into 3D facial structures. It provides clinicians and researchers the images to study and consider what is otherwise invisible or significantly distorted with traditional 2D X-rays. This high throughput machine provides immediate clinical interpretation to help diagnose and subsequently develop treatment strategies. Use of CBCT has significantly increased over the past few decades as patient exposure to radiation decreased and sometimes is comparable to 2D panoramic X-rays.

Panoramic X-ray is one type of 2D X-ray that orthodontists, pediatric dentists, oral surgeons, and other dental specialists have typically used. These types of X-ray units rotate around a patient's head and capture the entirety of the maxillomandibular complex (upper jaw, lower jaw, teeth, and surrounding tissues and structures) in one single image.

The radiation of this single panoramic X-ray can vary; there is more radiation than conventional periapical or bitewing X-rays which capture small areas of interest within a patient's mouth, but usually less than any type of CT imaging. Panoramic X-rays typically have a dose ~20 micro-Sieverts per image (Ludlow 2014). Radiation dose for CBCT varies significantly based upon certain parameters-some of which include the field of view, type of scan chosen, and machine used to capture images.

There have been numerous studies comparing 2D radiographs to tomograms from 3D CBCT imaging. 3D imaging provides better visualization and detection of

structures related to the craniofacial complex which cannot be clearly delineated in 2D radiographs. Comparisons were made between these two systems to assess the diagnostic accuracy of cortical erosions in the temporomandibular joint (TMJ). The observers were instructed to determine condylar defects based on structural changes (i.e., flat surface or irregularity deviating from normal condylar form) and/or changes in mineral density (i.e., lack of cortical bone). The observers exhibited higher reliability and accuracy with CBCT imaging compared to 2D imaging techniques (Honey et al. 2007).

Panoramic and CBCT images were compared for identification of the mandibular canal when it comes to presurgical dental implant assessment and in relation to third molars. CBCT imaging allowed for identification of the mandibular canal by reducing the inefficiencies in panoramic X-rays, which include magnification errors, superimposition of adjacent structures, geometric distortion, and other problems (Angelopoulos et al. 2008). These two systems were also compared in identifying the mandibular canal before 3rd molar extraction. The CBCT scan allowed clinicians to better appreciate the position of the canal relative to the third molars in comparison to panoramic X-rays (Ghaemina et al. 2009). It could be inferred that CBCT imaging would thus allow for a better idea of where teeth are in relation to the inferior alveolar nerve; this could result in a reduction of subsequent nerve injury during extraction of 3rd molars. CBCT scanning has become the standard of care for some procedures and allows for better risk assessment and enhanced surgical planning compared to panoramic radiography (Ghaemina et al. 2011).

These imaging modalities also were used to evaluate detection of external root resorption of lateral incisors resulting from ectopically erupting canines. It is often hard

to decipher whether canines have truly resorbed lateral incisors in one 2D image because of overlap and magnification errors. CBCT allowed for better sensitivity in detecting slight and severe root resorption cavities compared to panoramic radiography (Alqerban et al. 2009). This enhanced accuracy can allow for an effective treatment decision regarding space creation and force vectors during exposure and bond therapy to limit damage to adjacent teeth and tissues. Orthodontists align teeth in a way that straightens them and optimizes root position to handle occlusal forces. Accurate interpretation of root angulation is thus essential to optimize outcomes. Orthodontists compared post treatment mesio-distal root angulations between traditional panoramic X-rays and CBCT scans and found statistically significant differences between the two modalities (Bouwens et al. 2011). This should alert orthodontists to interpret panoramic X-rays with caution as accuracy may be compromised.

Another study compared diagnostic capabilities between 2D and 3D CBCT sialography and concluded that CBCT permitted enhanced gland visualization as it enabled delineation of pathology within detectable limits (Jadu and Lam 2013). This improved diagnostic ability helps plan appropriate treatment decisions and potentially allows for earlier and more effective treatment. Since this technology is still relatively new, there is much untapped potential within the wealth of information a CBCT image provides; not all information captured is viewed in traditional final images. It is highly probable that the information on a CBCT is underutilized. It would be useful to explore additional, reliable information from a CBCT. Efforts that focus on improvement of contemporary diagnostic tools can better patient care. Steps can be taken to combat

clinical failure rates and reduce negative outcomes by performing the appropriate research and analyses that may allow for enhanced utilization of CBCT images.

Imaging in orthodontics

Around the U.S., orthodontists typically use either panoramic 2D X-rays or CBCT imaging as part of the initial records process. They also take these images during treatment and at the end of treatment. The standard of care has traditionally been and is currently panoramic radiographs although the future seems to be trending towards CBCT imaging. The amount of information that can be gleaned from and the accuracy of 2D X-rays is more limited. CBCT imaging, on the other hand, captures a large amount of information. Some orthodontists only take CBCT scans when warranted to help establish a diagnosis and guide treatment. These could include aspects related to impacted teeth, surgical exposures and bonding of impacted teeth to facilitate proper eruption, patients with temporomandibular joint (TMJ) disorders, or complications that impact the jaw biomechanics.

CBCTs are used as diagnostic tools only because they are used on patients with symptomatic conditions. The primary purpose of a diagnostic tool is binary - to determine the presence or absence of disease which then would guide treatment. Diagnostic tools such as CBCT are useful in symptomatic individuals. It would be prudent to investigate, however, whether CBCT imaging could be useful as a screening tool. Some practices do utilize CBCT imaging on most patients thus making CBCT data a potential screening tool. The main purpose of a screening tool is to determine risk factors or detect early and potentially progressive pathologies/disease and is not

exclusive to symptomatic individuals; to be useful, the benefits of a screening test must outweigh the risks. As the trend in imaging within dentistry and more specifically orthodontics is leaning toward scanning every patient with CBCT, there lies the opportunity to extend its use as a screening tool. As a screening tool, it would allow us to potentially identify risk factors and/or pathology before symptoms arise. Furthermore, it can guide diagnoses and treatment decisions, which should significantly benefit patients and related outcomes.

In the absence of tapping into the potential of CBCT as a screening tool (patient radiation exposure [albeit less] has already occurred) we are not maximizing its full potential and in turn are shortchanging our patients of additional information and an optimized clinical treatment. As radiation exposure continued to decrease with betterment of technology, CBCTs can be safely obtained on most patients and the complete data can be analyzed to help screen for earlier stages of asymptomatic pathologies in addition to diagnosing and formulating treatment strategies for symptomatic conditions. It will be important, when it comes to imaging to continue to weigh the potential benefits (i.e. the extent to which there is a better diagnosis and treatment) of CBCT images against the potential costs (i.e. unnecessary radiation exposure) in order to establish the ideal standard of care.

Current and potential applications

With each CBCT scan in orthodontics, the location and angulation of the teeth are determined, lengths of roots are identified, bone height and bone width are viewed, sagittal and coronal TMJ sections are analyzed, and airway is observed. Initial

assessment and diagnosis are derived and qualified in all patients, and although this is thorough and comprehensive, it remains only qualitative. Images that are captured and diagnosed are based on the subjective opinion from the treating doctor(s). These opinions are typically formulated from comparing a mental repertoire of many different CBCT scans that have been previously evaluated. In most instances, these subjective diagnoses (i.e., the amount of bone surrounding teeth, length of roots, anomalous jaw joint structures, density of the jaws, airway measurements) may be correct and can identify multiple problems or lack thereof from the scan. However, there are many asymptomatic pathologies or early problems that may be overlooked or misdiagnosed. Examples of this include minimal bone surrounding teeth leading to an increased likelihood of periodontal damage, greater effects of root resorption, active remodeling and/or degenerative joint disease of the TMJ, inability to identify cysts or tumors within the jaws or near teeth, and inaccurate diagnoses of sleep conditions. This may be because of lack of true understanding of the structure and “quantified” densities of different components that comprise the maxillomandibular complex.

There is a lack of precise, quantitative measurements, and thus an absence of streamlined training curriculum. It should be a goal and point of emphasis to develop a thorough understanding of all maxillomandibular facial structures to effectively diagnose, and screen all patients who undergo CBCT imaging for accurate bone width and height, bone density and structure, root resorption, structural abnormalities of the TMJ, cysts or tumors, and detection of early stages of pathology. In order for CBCT images to be an accurate and valid screening tool to detect upstream events leading to a downstream pathological condition, however, one must first be able to accurately

quantify and interpret all images. One can expedite this process by programming deep learning algorithms in order to make it a more effective screening tool.

Radiography, tomography and clinical scenarios

Bone structure and bone density within the craniofacial complex could potentially have significant implications on clinical diagnosis, screening, and treatment as well as research. Radiodensity, traditionally measured by a Hounsfield unit (HU) and/or grayscale, could be used to determine mineral density for structures within a scan. HU is a dimensionless unit that is a relative quantitative measurement of radio density in CT scanning. The HU is determined by a linear transformation of the baseline attenuation coefficient of the X-ray beam – water is randomly designated as zero HU and air is - 1000 HU (DenOtter et al. 2019). Thus, the higher density of a specific tissue with more x-ray absorption, the brighter the image and more positive the HU value is. Tissue that is less dense tends to be darker and have more negative values. HU traditionally apply to medical-grade CT scan but not to CBCT scans. Whereas HU is proportional to x-ray attenuation by a tissue in CT scans, the degree of x-ray attenuation is demonstrated by gray scale, which is a voxel value, in CBCT scans (Razi et al. 2014).

For CBCT scans, the accuracy has been shown to be compromised since there is no good data relating grayscale or HU to mineral density. Many of the current CBCT systems are not standardized to density, and grayscale values between machines often tend to be arbitrary than exact CBCT machines and software often show grayscales as HUs, however, these are not truly HUs (Mah et al. 2010). Despite the disadvantages of CBCT machines which include high levels of artifacts and radiation scatter, some

studies have shown a linear relationship between HU in CT scan and gray scale in CBCT (Mah et al. 2010). The voxel gray values from a CBCT deviate from true HU units but since a linear relationship exists, HU units from CBCT can be derived from predictive models (Parsa et al. 2012). Several studies have attempted to convert CBCT gray values to density measurements via HUs and have found positive correlation between HU from a multislice CT (MSCT) scan and from CBCT scan (Aranyarachkul et al. 2005; Naitoh et al. 2009; Reeves et al. 2012; Cassetta et al. 2013). Large amounts of scattering and artifacts, however, have hindered the reliability of CBCT scans in specific types of measurements like bone mineral density. CBCT scanning has improved for certain measures of bone quality like bone volume fractions and certain microstructural assessments, but the accuracy of bone density has continued to remain a problem (Parsa et al. 2015).

Through standardization and calibration, CBCT systems could get to a point in which radiodensity and thus mineral density become a more accurate measurement. Understanding the numeric value and distribution of bone density could allow for a more holistic approach to research and clinical decision making. Effects of adaptation of the skeleton to its biomechanical environment could be further elucidated. Changes in bone density over time could indicate changes with growth and/or pathological processes. Exact bone measurements could help with dental implantology planning, placement, and healing. Bone density was found to be directly related to strength of bone before microfracture (Misch 1990). There was sometimes a tenfold difference in bone strength as one progresses from the densest bone (D1) to least dense bone (D4) in the maxillofacial complex. To minimize bone microfracture during mini implant placement,

stress should be reduced in lower density regions. Thus, precise identification of bone density throughout the jaws is necessary for implant stability and success. Insertion torque should be minimized in higher dense regions which can be accomplished with a pre-drilling method. Placement of implants in D4 bone can have high implant failure rates, up to 50% failure, therefore it may be prudent to identify alternative methods of treatment with a higher chance of success (Kravitz et al. 2007).

Type, duration, and direction of tooth movement could be more easily predicted. There tends to be inverse relationship between rate of tooth movement and bone density. Mandibular molars are surrounded by denser bone compared to maxillary molars and adults which usually have denser bone than children. This knowledge is very important since tooth movement can occur at a faster rate in areas of lower bone density and based on desired movement, orthodontic anchorage may need to be augmented (Chugh 2013). These are just a few of the ways in which better knowledge of different maxillofacial structures and densities can have a profound impact on implant success, tooth movement, anchorage loss, and risks/side effects during treatment (Chugh 2013).

Dental implants have become more popular over the years and on a whole, it appears that implant success has improved but many of the studies are shorter terms looking 1-5 years post implant placement. When an implant does fail, often, we are unaware as to the reason behind its failure. There are some known risk factors for implant failure, but there are many unknowns. Long-term success of implants is influenced by the quantity of bone available from a mesial distal and from a buccal lingual direction as well as the quality of the bone. The general assumption is that the

thicker and denser the bone, the higher rate of success. But the thickness and bone mineral density for the most part has only been qualitatively described even with the increased use of CBCT imaging. This study used Lekholm and Zarb's classification of bone density, describing bone into the four types: Q1, 2, 3, 4. Q2 is most popular in the mandible and Q3 dominated the maxilla. The results of the study showed that in order of density: anterior mandible > posterior mandible > anterior maxilla > posterior maxilla. The implants most likely to be mobile at placement were Q3 and Q4. This knowledge has helped dentists, surgeons, and other dental specialists place implants and predict stability but it is still not an optimized system as the cut off between each of these regions is qualitatively described (Truhlar et al. 1997).

In addition to stability of implants related to density, other studies have shown that bone quality, implant geometry, and drilling sequence influences primary stability of implants (Voumard et al. 2019). To be able to correctly assess bone density and other factors more precisely, important insight can be gained as to type and method of implant placement. Routine CBCT scans can provide very valuable information for stability and success of implants. With accurate bone mineral density measurements and long-term studies evaluating implant failure and success, dentists can better determine likelihood of success and optimize strategies to achieve that. Dental professionals can accomplish more predictable and stable results.

Bone mineral density measurements

Over the years, a variety of methods have been used to assess bone mineral density: radiogrammetry (RG), Compton scattering technique, radiographic

photodensitometry (RP), single energy photon absorptiometry (SPA), dual-energy photon absorptiometry (DPA), neutron activation, quantitative computed tomography (QCT), dual-energy X-ray absorptiometry (DXA), and panoramic X-rays. Each of these techniques has pros and cons associated with them and some are more widely used than others. Since the field of dentistry primarily uses intraoral X-rays, panoramic X-rays, and more recently CBCT imaging, it would be ideal to precisely determine bone mineral density using this type of imaging. Panoramic X-rays were used to evaluate bone mineral density but much of the density is based on subjective interpretations from the observer with no real value associated with the bone (Chugh 2013). It would benefit patients and clinicians to have a more objective measurement for bone mineral density and other vital structures within the maxillofacial complex.

Traditionally in dentistry, bone quality had been assessed with 2D radiographs and observations from the clinician. Several different bone density classifications have arisen over the years. One of the most widely used methods subjectively describes and places bone into one of four types: Type 1-dense homogenous cortical bone with small trabecular core; Type 2-large, dense layer of cortical bone surrounding dense trabecular core; Type 3-thinner layer of cortical bone around dense trabecular core; and Type 4-thin cortical layer surrounding low-density trabecular core (Lekholm & Zarb, 1985). Another method described to assess bone quality has been separating bone mineral density by HUs. This classification system corresponds to five groups, ranging from values less than 150 to values greater than 1250 (Misch et al. 1999). The cutoff between each of these 5 groups was relatively arbitrary and there was not much clinical significance tied to them, so this classification system is rarely used. There is much

more potential, however, regarding the use of grayscale and HU as a measurable and significant tool for measuring density of various structures within the maxillofacial complex.

Micro X-ray computed tomography

One of the higher resolution scanners that is often used as the gold standard for many pathological investigations is the micro X-ray CT (Micro XCT). Micro XCT is capable of acquiring images at a very high resolution in which the fine external and internal structures of objects can be viewed. The small x-ray source illuminates the object being scanned and a detector collects hundreds of magnified images as the object rotates. Micro XCT provides markedly improved scanning quality by detecting changes in structure and mineral density within volumes of scanned tissues. Micro XCTs are typically used to investigate pathologic material excised from patient/animal models (e.g. excised bones, extracted teeth) at a much higher resolution. A major limitation of micro XCT is lack of contextual information (i.e., adjacent tissues/structures). Micro XCT cannot be used with our patients, however, data obtained from such images can be extrapolated to more traditional imaging modalities to improve upon their utility. By comparing and contrasting calibration specimens across CBCT and Micro XCT imaging systems, one may be able to more reliably interpret images taken on a CBCT scanner.

More recent studies have analyzed mineral density volume gradients using normal and disease human tissues with micro XCT imaging. There are relatively accurate estimates of density variations for several structures within the human

maxillomandibular facial complex: enamel, dentin, cementum, bone, calculus, etc (Djomehri et al. 2015). These mineral density gradients establish a baseline number by which to compare normal and pathologic processes. The key, however, is to calibrate the micro XCT scans to CBCT scans so these measurements can be accurately captured on imaging systems which are readily to investigate structures on a macro level (ex: maxillomandibular complex).

Calibration of scanners for quantitative measures of mineral density

The purpose of this investigation is based on the motivation that, with systematic, reproducible calibration of structure and mineral density, from micro XCT and contextualized to CBCT, differences within tissues can be more accurately resolved. This calibrated system can then be used to enable expanded screening and an effective diagnostic tool, with a central objective to increase the standard of patient care. Enhanced calibration and higher resolution radiographs will help improve our understanding of pathophysiologic processes and help identify new potential therapeutic targets for both researchers, clinician scientists, and clinicians. In this study, systematic calibration of three CT systems using calibration specimens of known mineral density was performed as a first step to gather insights into the use of a CBCT. Development of a CBCT scanner calibrated for both structure and mineral density will expand their use to enable to be used as a screening tool (in addition to being a diagnostic tool) for individual treated by dentists.

We **hypothesize** that correlating calibration curves across length scales from X-ray micro computed tomography (microscale) and clinical care CBCT (macroscale) will

allow contextual visualization and an accurate mineral density map of pathological biominerals. There are three **main objectives** to this study: 1) For known mineral densities of a phantom and hydroxyapatite, identify the grayscale value associated with it to create a calibration curve; 2) Contextualize MD of human tooth and surrounding structures, namely tissues of human jaw. Compare to MDs of same material from microXCT scan; 3) Extract mineral densities from CBCT scans using experimental groups.

Materials and Methods

Computed tomography (CT) systems

Three different types of CT scanners were used to help achieve the goals of this project: two CBCT scanners (CBCT 1 and CBCT 2) and one micro XCT scanner. Each scanner has different specifications and energy thresholds as shown below in Table 1.

Table 1: Scanning parameters of computed tomography (CT) systems, cone beam CT 1 (CBCT 1), CBCT 2, and Micro X-ray CT (Micro XCT)

	CBCT 1	CBCT 2	Micro XCT
Type	Carestream CBCT CS 9300	Carestream CBCT CS 8100	Zeiss MicroXCT-200 (4X)
Location	UCSF Dental Center	Private Practice	BBCMC, UCSF
Field of View (cm²)	11 x 17	8 x 9	0.5 x 0.5
Unit	Greyscale	Greyscale	Greyscale, HU, and Mineral Density (mg/cc)
Voxel size (µm)	250 x 250 x 250	150 x 150 x 150	5 x 5 x 5
Current (mA)	4	4	0.198
Voltage (kVp)	90	84	40
Effective dose	Dose area product (DAP): 897 mGy.cm ² Fast Scan: ~142 µsv	1169 mGy.cm ² Fast Scan: ~45 µsv	~800 µsv

Calibration of three CT systems

Each scanner was first calibrated to a set of known mineral density phantoms. Intensity indicative of X-ray attenuation in relation to mineral density in respective phantoms were analyzed to provide a correlation for all X-ray CT systems. A calibration curve would be created such that we gather as much information equivalent to a micro XCT on CBCT machines (CBCT 1 and CBCT 2). In order to start the calibration process, it was necessary to image the same object with all machines. Two phantoms (small and large phantoms) were fabricated, of known shapes and mineral densities; concentric cylinders containing known mineral density segments of 0, 100 250, 500, and 750 mg/cc (Figure 1). These were proprietary phantoms constructed by CIRS Tissue Simulation & Phantom Technology. The entire small and large phantom were scanned using the CBCT 1 (Carestream CBCT CS 8100, Carestream Dental LLC, Atlanta, GA, USA) and CBCT 2 (Carestream CBCT CS 8100, Carestream Dental LLC, Atlanta, GA, USA), whereas only one block of small phantom was scanned using micro XCT (MicroXCT-200, Carl Zeiss X-ray Microscopy, Pleasanton, CA, USA) to accommodate a much smaller field of view (Figure 1). Hydroxyapatite of various sizes (small, medium, and large) of known mineral density (3000 mg/cc) were separately scanned using the micro XCT and CBCT 1 in order to calibrate high mineral density materials.

To construct calibration curves of different CT systems, CT images of the same phantom were segmented by extracting subvolumes for each layer (0, 100, 250, 500, 750mg/cc, schematics of phantom design) based on the length from the bottom of the image using Avizo software (Thermo Fisher Scientific Inc., Hillsboro OR, USA). Average gray value of each segmented phantom layer was plotted against known MD value of

corresponding layer. Gray values of hydroxyapatite (HA, 3000 mg/cc) were added to the calibration graph. Structural and mineral density (MD) maps were used to correlate X-ray intensities across systems: phantoms, hydroxyapatite, and human mandibles.

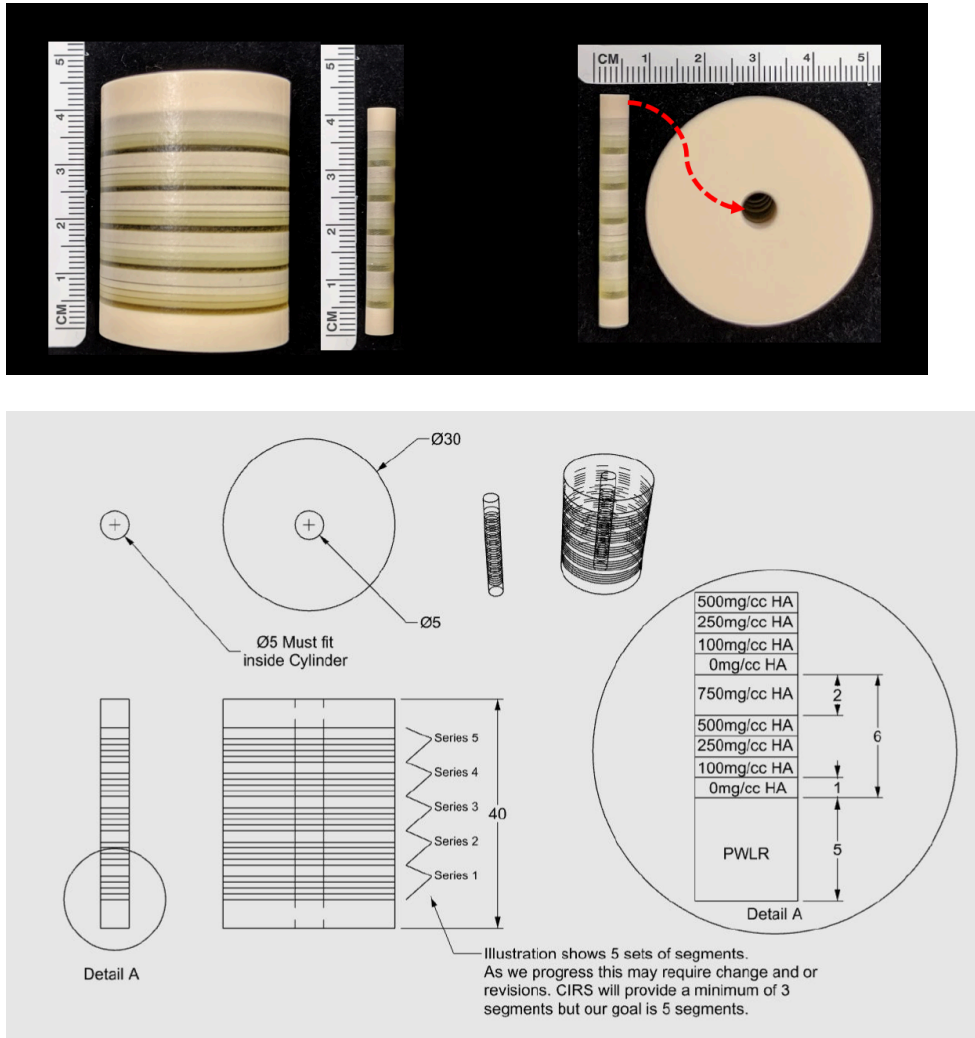


Figure 1: Large phantom and small phantom (top row), concentric cylinders containing known mineral density segments of 0, 100 250, 500, and 750 mg/cc.

Specimens and comparison of MDs

An entire mandible from the UCSF Willd Body Program was scanned using CBCT 2 with specification as indicated above. The same mandibular incisor was selected for analysis with CBCT 2 and micro XCT. In order for the mandibular incisor

and bone to be imaged with the micro XCT machine, the tooth and part of the jawbone were removed from the human mandible. Soft tissue surrounding the incisor was removed and the bone surrounding the teeth was sectioned. The incisor remained intact with some residual bone attached to the root. After sectioning, the incisor was scanned using the micro XCT.

5 patients' CT data using CBCT 1 were selected from a pre-existing database of CT images taken during routine diagnostic records at the University of California San Francisco orthodontic clinic. These images were used following the Institutional Review Board approval at the University of California, San Francisco (protocol # H8933071801). Each of these images were scanned using the same scanner and same settings as used with the phantoms and hydroxyapatite. These were all females (n=5, age range 28-74 y/o) without known history of medical complications.

To compare MDs between CBCT 1, CBCT 2, and micro XCT systems, the mandibular right incisor region was selected and enamel, dentin, cortical bone, and trabecular bone were segmented manually by structure using the AVIZO software. MD values were determined based on calibration curves and box plots and histograms of MDs of enamel, dentin, cortical bone, and trabecular bone of each system were compared.

To compare CBCT 1 patient data, mandibular right canine tooth regions were identified and analyzed for MDs of enamel, dentin, cortical bone and trabecular bone in each individual. Restorations, implants, and other suspected pathology was analyzed in each of these individuals.

Size and shape effects on mineral density

Different sizes and shapes of phantoms and HAs were imaged using CBCT 1 and micro XCT. The phantoms were the same as used above with increments of mineral density from 0 to 750mg/cc and the segment used was 145mm³. The HA came in three sizes: small (16 mm³), medium (77 mm³), and large (467 mm³). Standard error (SE) of MD were plotted against surface area to volume ratio.

Results

Scanned phantoms from each of the CT machines can be visualized with heat maps in Figure 2. Each mineral density layer is represented by a different color based upon the value of the voxel grayscale. Different mineral density layers were distinct, clear, and easy to distinguish on the small phantom scanned with the microCT. The mineral density layers, however, were not as clear and overlapped for patient care CBCT systems. The differing grayscale values and resolution allowed for some distinguishing of layers, but bleeding of colors was observed in all CBCT scanned phantoms. Average gray scale of subvolume of each layer was determined and plotted against known mineral density value of each phantom layer, as displayed. Calibration curves show that values between CBCT systems and micro XCT have very different grayscale readings even at known mineral density. Slopes of the curves vary sharply in magnitude and steepness. Plot profiles reveal that the CBCT scans do not show clear steps of each mineral density layer. Micro XCT clearly separates each step with enough data points indicating the reliability of deciphering each layer of the phantom.

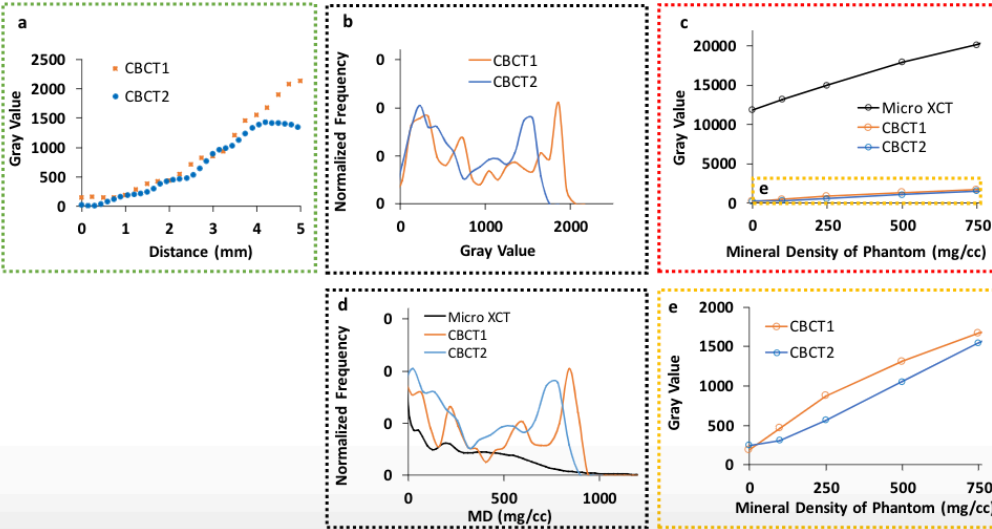
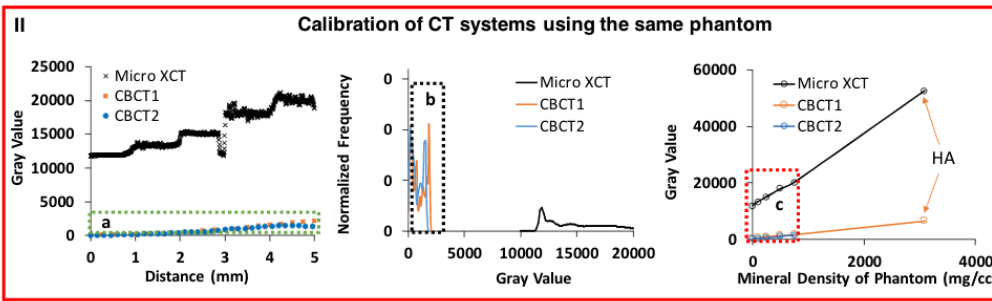
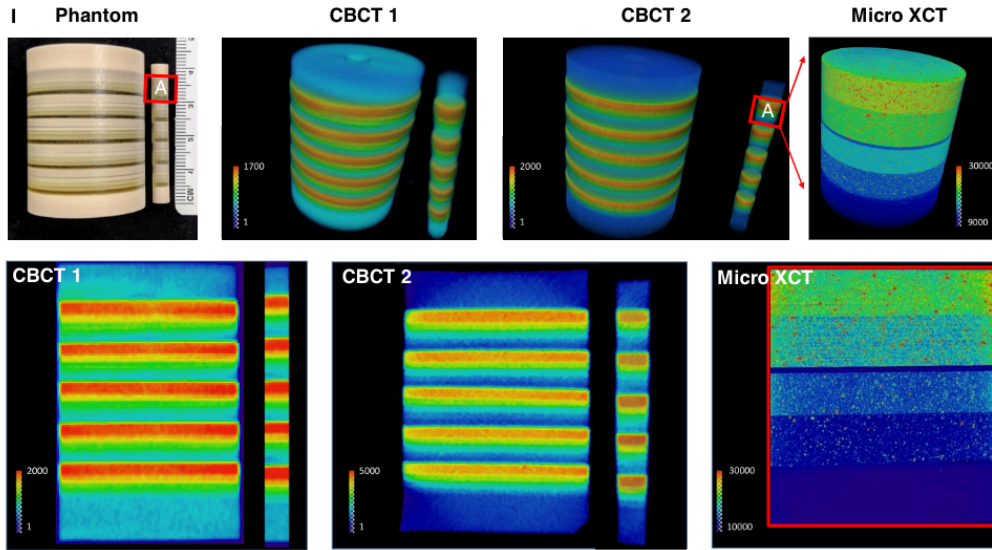
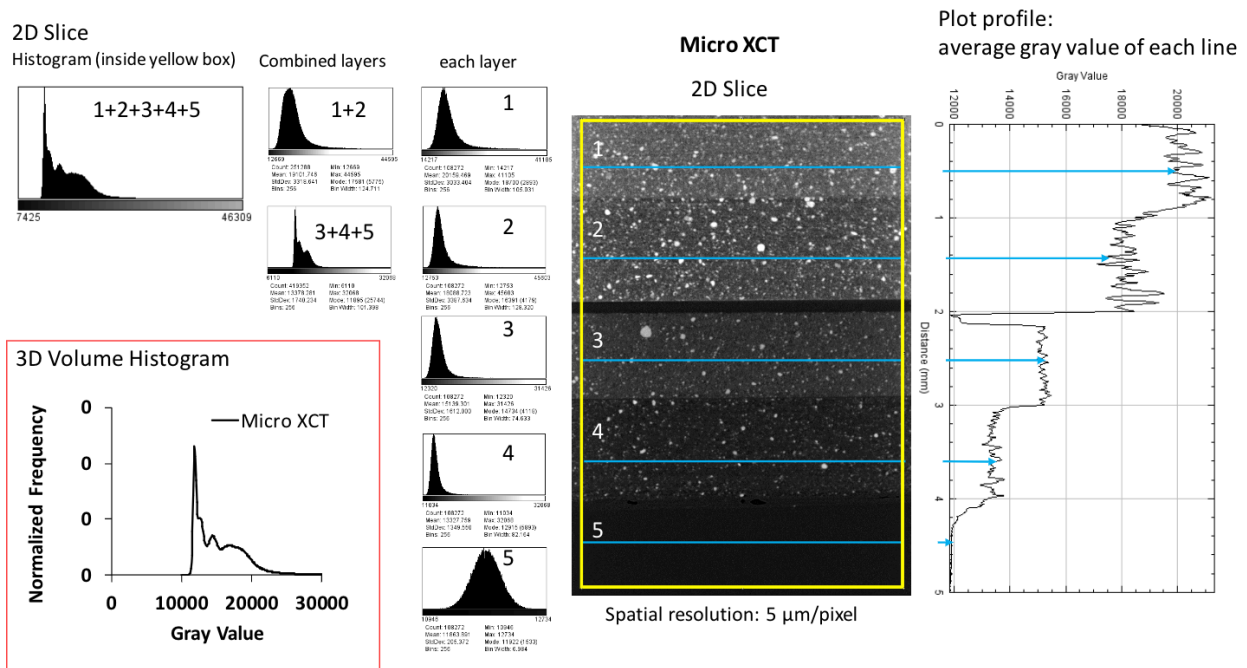


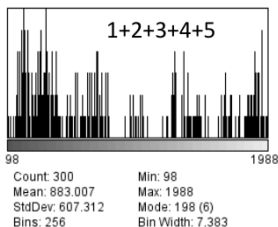
Figure 2: Calibration of computed tomography (CT), CBCT 1, CBCT 2 and micro X-ray CT (Micro XCT). I). Top row illustrates larger and smaller phantoms. The smaller phantom was imaged in all CT systems. The larger phantom was imaged only in CBCT 1 and CBCT2. 3D (top row) and 2D (second row) Gray Value heat maps of the same phantom scanned from each CT system (CBCT 1, CBCT 2, micro XCT) show different mineral density layers (MD). *Note: Gray Value differences in color map between two CBCT systems and micro XCT. **II).** Gray Value profiles (left graph) taken along the phantom length of the region in the red box (I, A). Orange (CBCT1) and blue (CBCT2)

profiles do not differentiate between the visually apparent different MD layers (I, A). Distinctive MD layers represented in black were apparent using a Micro XCT. Histograms (middle graph) illustrate that Gray Values for both CBCT 1 and 2 are within a narrower range compared to a broader range for Micro XCT (detailed illustration in figure 2). Calibration curve of Gray Value plotted against known MD value of each phantom layer is shown (right graph). Note: hydroxyapatite (HA) were scanned separately (figure 6) and were added to the calibration graph (right graph). Additionally, regions a, b, c in graphs in row three are elaborated as plots a, b, and c in the fourth row. MD histograms (d, row 5) were plotted after converting Gray Values into MD and an enlarged view of region e in the calibration graph illustrates the differences in two CBCT systems. CBCT systems diverge from micro XCT data starting around 250 mg/cc (enlarged view of b).

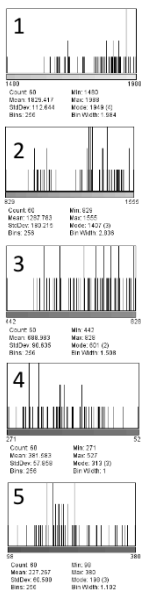
A further analysis of the grayscale distribution of each scanned phantom was completed and plotted as seen in Figure 3.



2D Slice Histogram (inside yellow box)

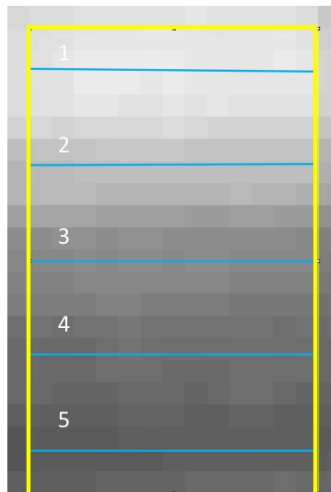


each layer



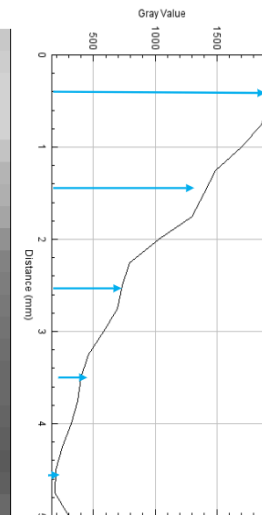
CBCT 1

2D Slice

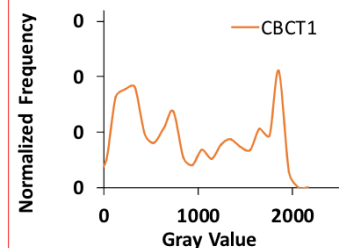


Spatial resolution: 250 μm/pixel

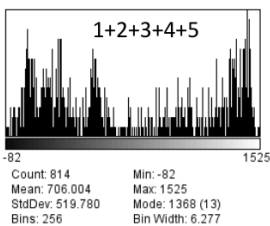
Plot profile: average gray value of each line



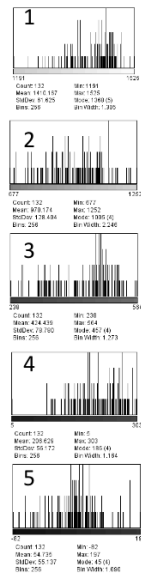
3D Volume Histogram



2D Slice Histogram (inside yellow box)

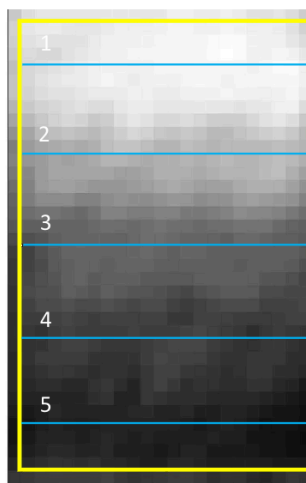


each layer



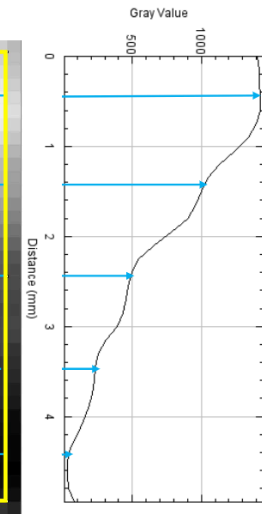
CBCT 2

2D Slice



Spatial resolution: 150 μm/pixel

Plot profile: average gray value of each line



3D Volume Histogram

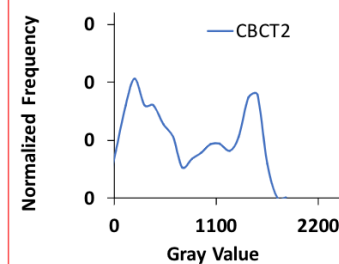


Figure 3: Phantom Gray Value distributions and plot profiles of MD layers of 0, 100, 250, 500, and 750 mg/cc using different CT systems. Micro XCT: all layers display normal distribution of Gray Values and the combined histogram of the 1 (750mg/cc) and 2 (500mg/cc) layers has one combined peak, so overall the 2D slice and 3D volume histograms show 4 distinct peaks of phantom. CBCT 1: 2D slice image is pixelated and there are mixed Gray Value regions between the different mineral density layers. The histogram of each layer is scattered and not normally distributed. Overall, 2D slice and 3D volume histograms illustrate more than 5 peaks. CBCT 2: 2D

slice image is less pixelated than CBCT 1 and shows the mixed Gray Value regions between the different mineral density layers. Histograms of each layer show scattered and non-normal distribution of Gray Values, and multiple peaks are observed in the overall 2D slice and 3D volume histograms. The sample size (or resolution) of CBCT systems are not sufficient to delineate the different mineral density layers.

Grayscale values were normally distributed in the phantom imaged with the micro XCT but not with the phantom imaged by CBCTs. This corresponded to easily distinguishable peaks with the micro XCT but no clear peaks with the CBCT machines. The increased voxel size and decreased quality of the images makes it difficult to definitively determine mineral density and when mineral density changes.

After establishing calibration curves among all three machines, these curves were used to compare and analyze multiple mineral density measurements of lower incisors. The images and sliced segments can be seen in Figure 4, along with the graphical and numerical measurements of enamel, dentin, cortical bone, and trabecular bone.

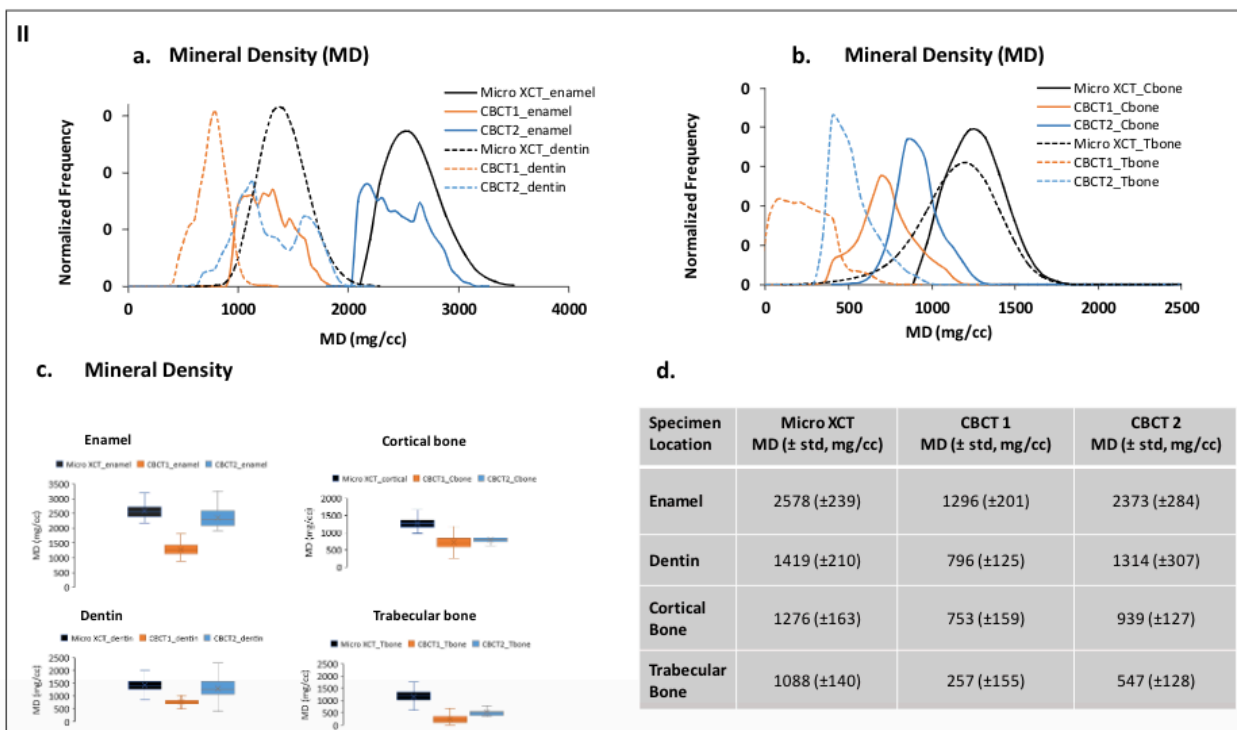
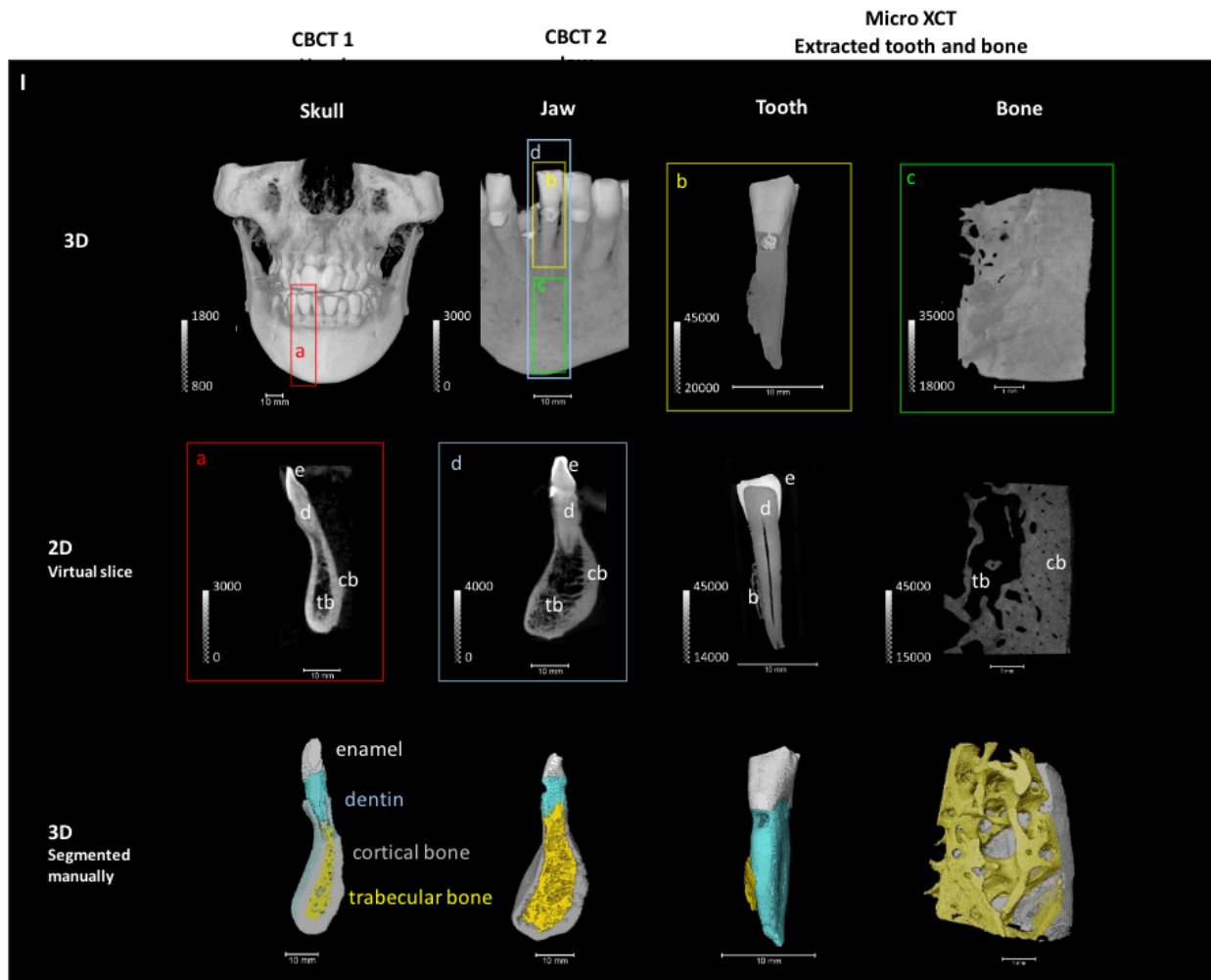
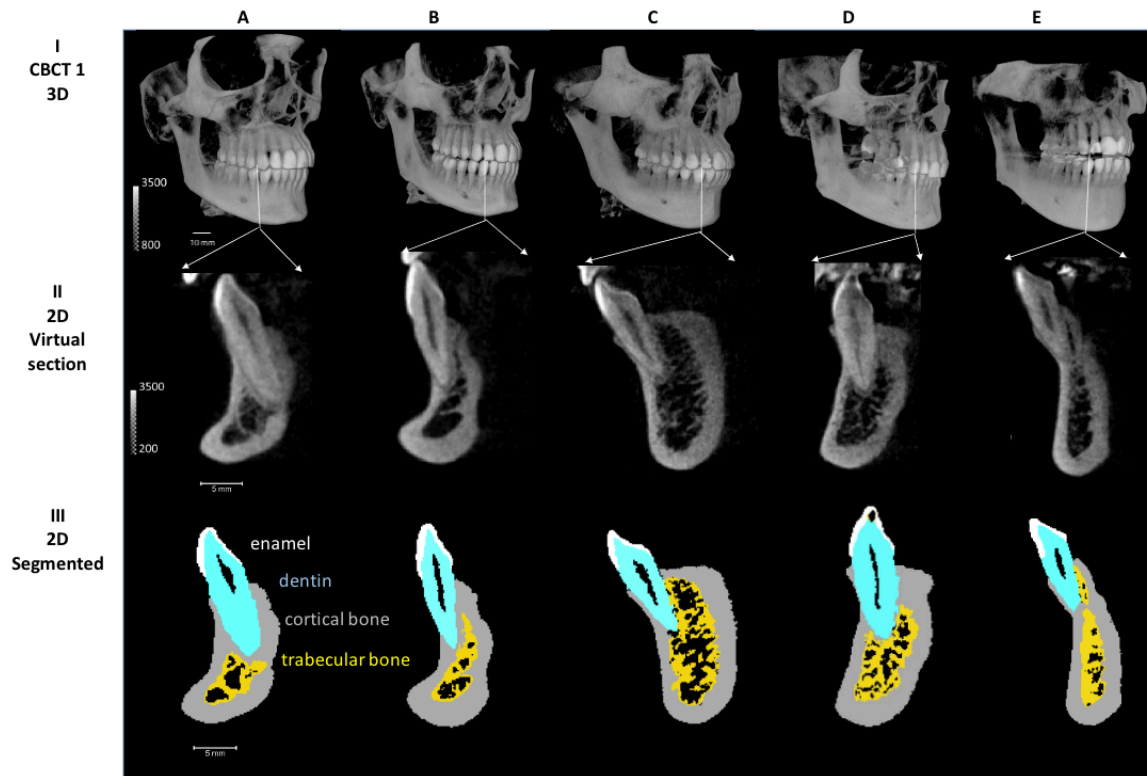


Figure 4: Comparison of mineral densities between CBCT 1, CBCT 2 and Micro X-ray CT. I). First row represents 3D volume rendered images of skull (CBCT1), jaw (CBCT2), tooth (b) and bone (c) (Micro XCT). Second row are 2D virtual slices of the corresponding 3D images in the first row. Second row highlights the enamel (e), dentin (d), cortical bone (cb) and trabecular bone (tb) as observed by all three CT systems. Third row illustrates manually segmented mineral density (MD) volumes that include white (enamel), blue (dentin), gray (cortical bone), and yellow (trabecular bone). **II).** Fourth row shows histograms of MDs for enamel and dentin (a, left) and cortical bone (Cbone) and trabecular bone (Tbone) (b, right) using all three CT systems. Gray Values from all CT systems were converted to MD values using calibration curves as shown in Figure 1. Histograms from respective CT systems illustrate normal distribution of MD values for Micro XCT only (black curves). MDs of enamel, dentin, cortical bone, and trabecular bone evaluated from each imaging system are shown in box plots (c, fifth row left). Corresponding numeric values of MDs are displayed in table d (fifth row right). Enamel and trabecular bone demonstrated large differences in MD measurements. Overall CBCT 1 has the lowest MD values compared to CBCT2 and Micro XCT.

Mineral density (from converted gray values) of enamel, dentin, cortical bone, and trabecular bone were plotted on a histogram for each system. The values are not normally distributed for either CBCT scan although the cortical bone for CBCT 1 and CBCT 2 is close to normal distribution. Enamel and trabecular bone measurements from CBCT 1 were the farthest off from the micro XCT. Values of enamel, dentin, cortical bone, and trabecular bone differed extensively between all systems even with the calibration curve. Values of enamel ranged from 1296 (\pm 201) mg/cc in CBCT 1, 2373 (\pm 284) mg/cc in CBCT 2, and 2578 (\pm 239) mg/cc in micro XCT. Values of dentin ranged from 796 (\pm 125) mg/cc in CBCT 1, 1314 (\pm 307) mg/cc in CBCT 2, and 1419 (\pm 210) mg/cc in micro XCT. Values of cortical bone ranged from 753 (\pm 159) mg/cc in CBCT 1, 939 (\pm 127) mg/cc in CBCT 2, and 1276 (\pm 163) mg/cc in micro XCT. Values of trabecular bone also varied all three machines ranging from 257 (\pm 155) mg/cc in CBCT 1, 547 (\pm 128) mg/cc in CBCT 2, and 1088 (\pm 140) mg/cc in micro XCT.

Mineral density measurements were then performed on five pre-existing CBCT images. The mid-section of the mandibular right canine was analyzed for each scan via a virtual 2D slice and segmentation as shown in Figure 5.



MD (mg/cc)	A	B	C	D	E	Average
Enamel	1129 (± 312)	1275 (± 316)	1178 (± 387)	916 (± 321)	931 (± 321)	1086 (± 330)
Dentin	815 (± 136)	873 (± 136)	757 (± 155)	770 (± 167)	677 (± 140)	778 (± 147)
Cortical bone	758 (± 198)	752 (± 173)	643 (± 207)	650 (± 191)	661 (± 214)	693 (± 197)
Trabecular bone	429 (± 104)	367 (± 202)	284 (± 120)	262 (± 117)	317 (± 172)	332 (± 143)

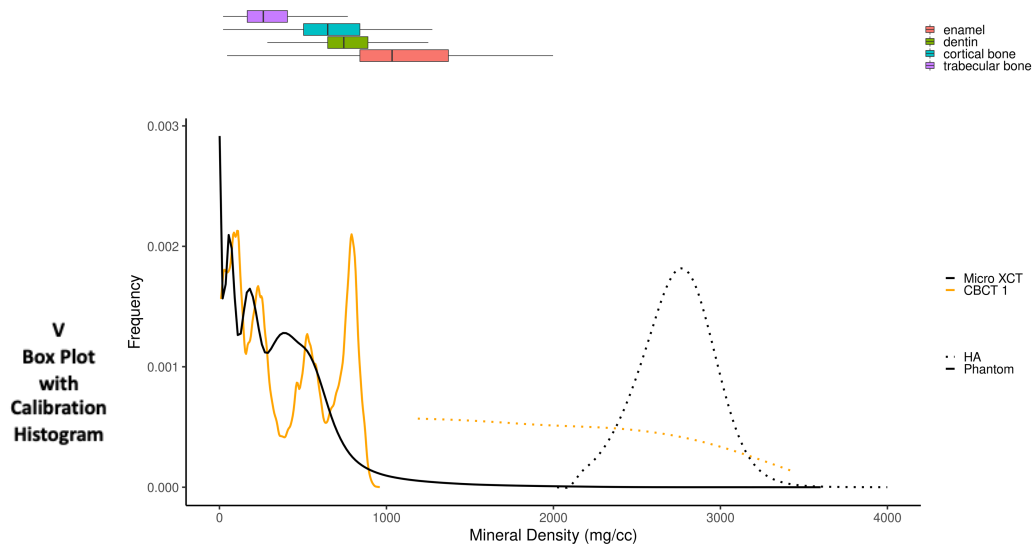
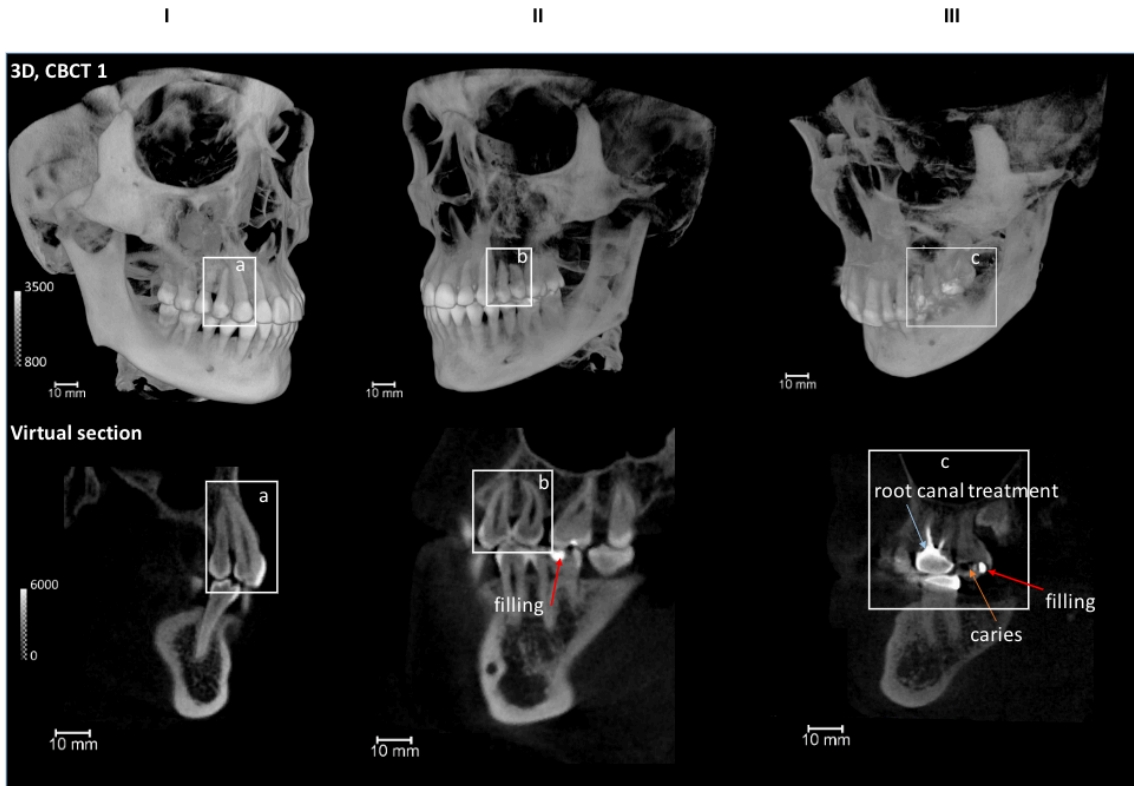


Figure 5: MD differences of canines of patients using CBCT 1. 3D volume rendered images using CBCT 1 (top), the virtual section of the mandibular right canine (middle), and colored section manually segmented by structure (bottom) – white (enamel), blue (dentin), gray (cortical bone), and yellow (trabecular bone). The box plots and table display MD differences of canines using CBCT 1 scan. Enamel shows the largest variance compared to other locations. Patients A and B have relatively higher MD values compared to patients D and E.

Three of the images were further analyzed to detect structural defects, existing dental treatment, potential dental disease, and bone density differences. This is illustrated in Figure 6.



IV Caries, filling, bone and implant

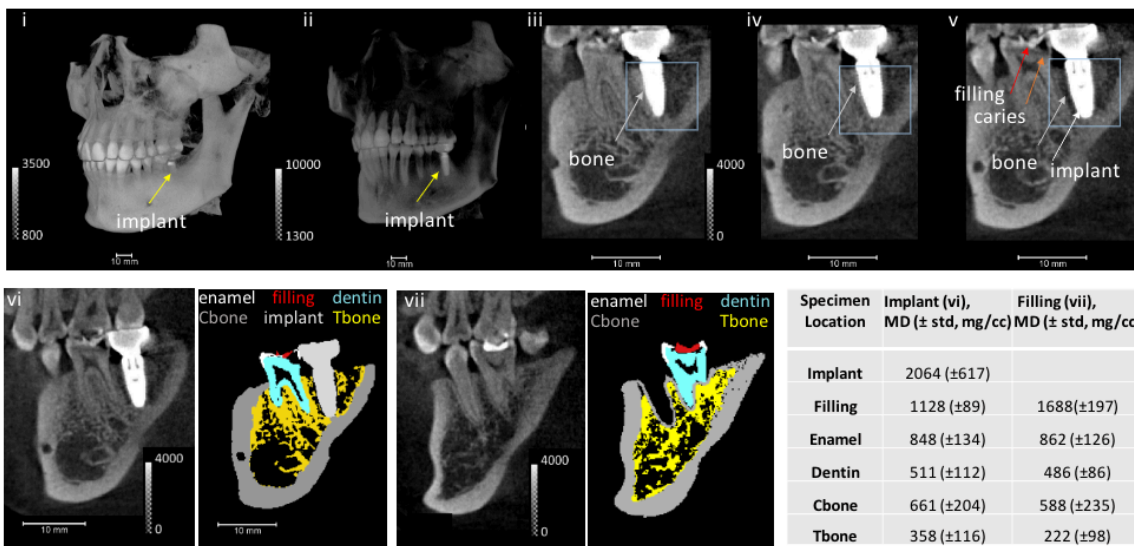


Figure 6: Analysis of structures and materials of different CBCT Images. Structural defects (white box, I-a and II-b), root canal treatment (III-c), filling (red arrows, II to IV), possible caries (orange arrows, III to IV), and bone density changes (gray arrows, IV) as seen by CBCT 1. The degree of osseointegration of dental implants (IV) are varied at different angles of view (IV-iii to IV-v, blue box). Teeth and bone surrounding implant (IV-vi) and filling (IV-vii) areas were segmented and resulted in relatively lower enamel, dentin, cortical bone MDs compared to the values from canines of patients (Fig. 4).

Structural defects, filling, root canals, osseointegration of dental implant, and caries were tentatively identified based on subjective opinion. These apparent findings were identified and labeled. Mineral density measurements were also made for several components of each segmented slice. These values are all lower than the mineral density measurements as described surrounding the canines.

In attempts to discover and explain why MD measurements have been inconsistent and inaccurate, effect of the magnitude of MD and size of specimen was explored further. Hydroxyapatite (HA) of known MD of three sizes (small, medium, and large) were scanned with the micro XCT and CBCT 1 to test the effect of MD level and size on the accuracy of MD. This effect is demonstrated in Figures 7 and 8.

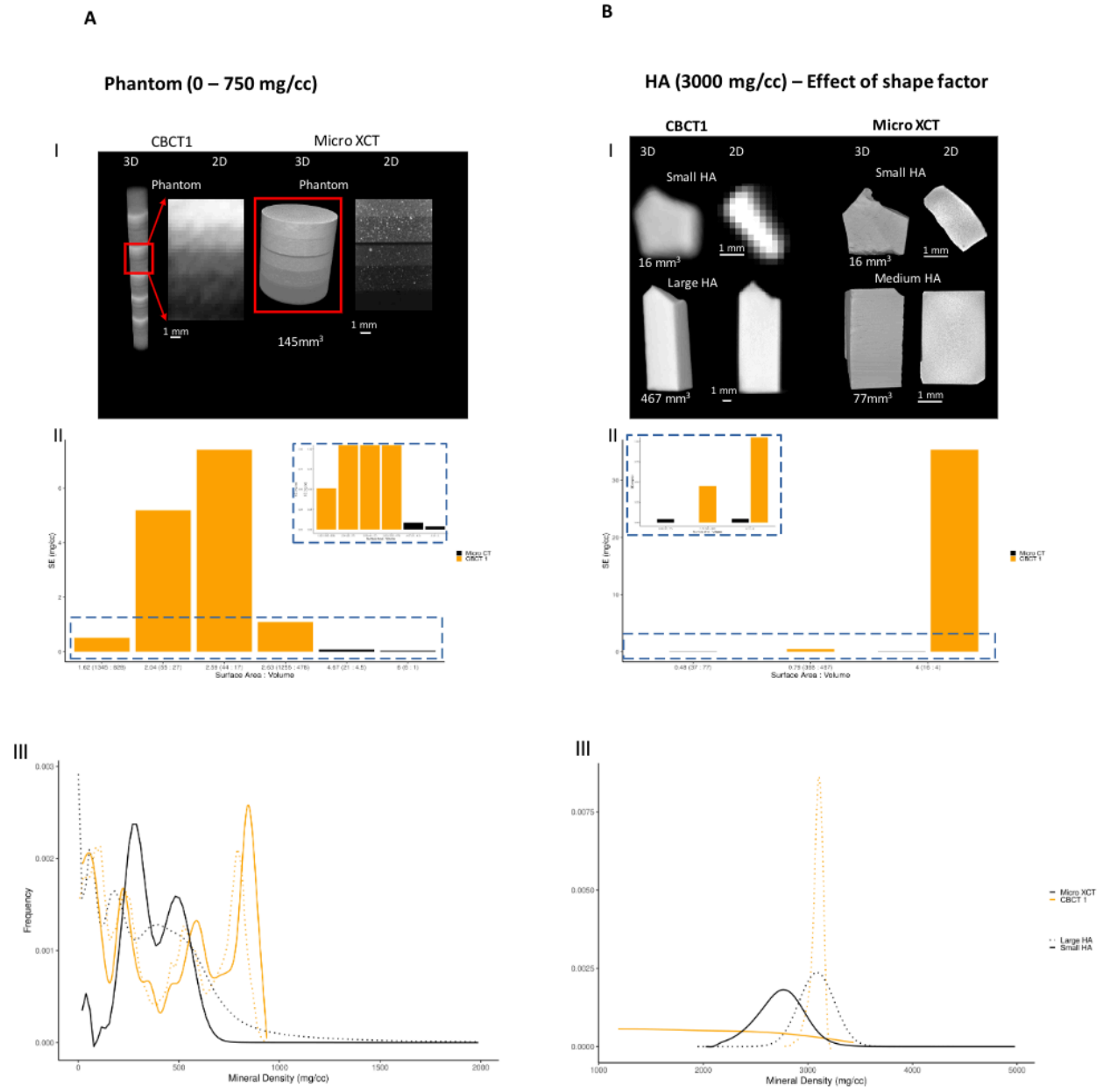


Figure 7. Size and mineral density dependent signals as seen by CBCT and Micro XCT systems. (A) Mineral density distribution of phantom from Micro XCT (solid black line) and CBCT 1 (solid yellow line) illustrate multiple peaks in the lower MD region. In MD regions less than 250 mg/cc (red box, also see inset), micro XCT illustrated more granular (higher resolution) measurements through three peaks compared to two peaks from CBCT 1. **(B) For specimens with higher mineral density, greater than 2000 mg/cc,** micro XCT shows a definitive signal also at higher MD regions with hydroxyapatite (HA) (solid line) as the calibration specimen. CBCT 1 with the same material (HA) shows a size dependent signal (Figure 7) of the calibration specimen.

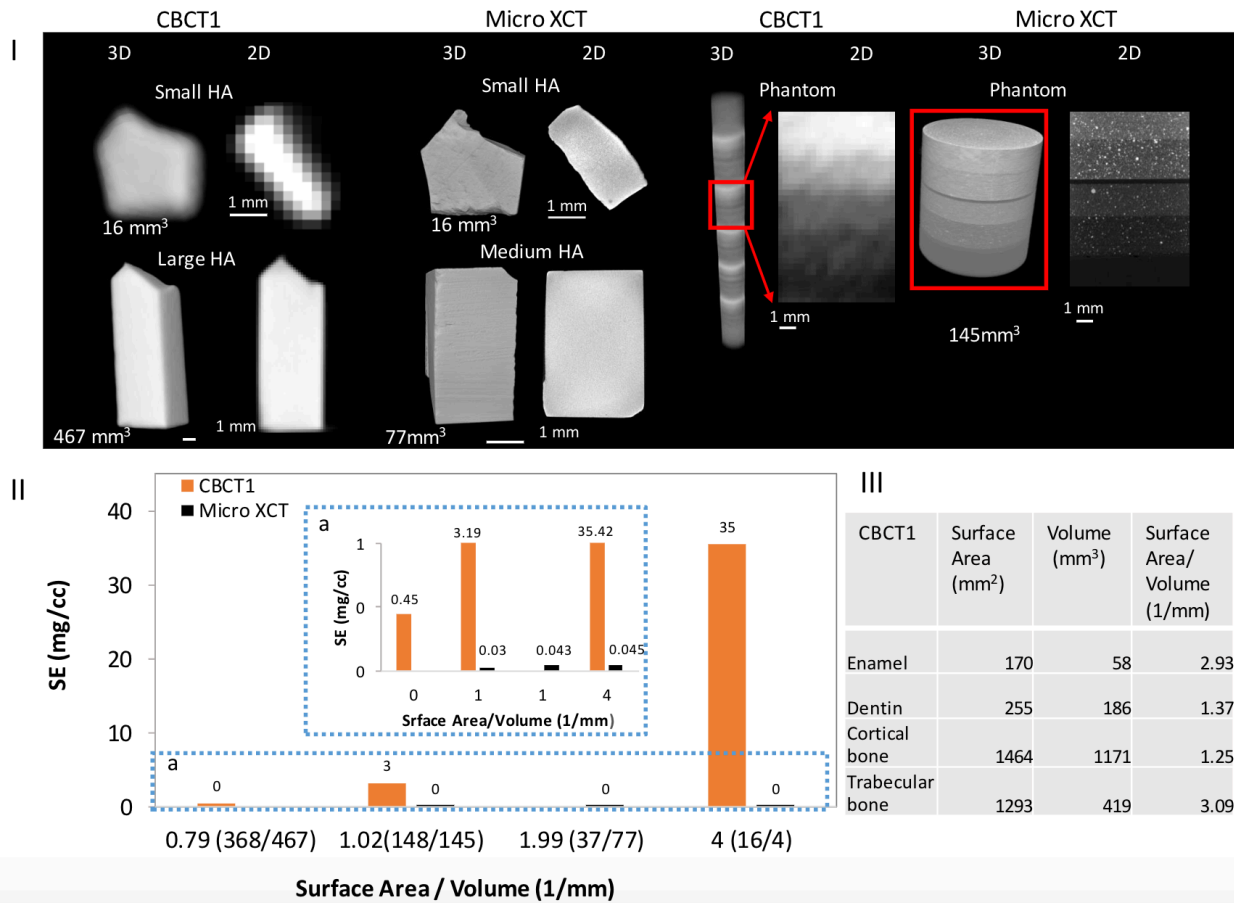


Figure 8: Size dependent signal of hydroxyapatite (HA) calibration specimen. I).

Different sizes of HA were imaged using CBCT 1 and micro XCT. Images using CBCT 1 are much blurrier around edges compared to micro XCT system, with the smaller sizes being blurrier and more pixelated. **II).** Standard error (SE)* of mineral density (MD, mg/cc) of each HA was plotted against surface area to volume ratio. The surface area to volume ratio decreases as the size of HA increases. The CBCT 1 system showed a consistently higher standard error of mean across both a small and a large calibration specimen when compared to Micro XCT system. Micro XCT system showed similar error between a larger and a smaller specimen, whereas the CBCT 1 system showed a large increase in standard error for a smaller specimen.

*Standard error is a measure of standard deviation of sample mean and is equivalent to full width at half maximum (FWHM). Under normality assumptions: $FWHM \approx 2.355 \cdot \sigma \approx 2.355 \cdot SE \cdot \sqrt{n}$

At smaller MD regions (<750mg/cc), there tends to be a high standard error for all values of phantom scanned with CBCT, whereas the standard error of measurements for the phantom under micro XCT is minimal. This was consistently the case for almost all MD measurements from CBCT. At higher MD regions (3000 mg/cc),

the micro XCT had a clear signal with all specimens with one peak whereas the CBCT1 showed a size dependent signal.

The effect of size of the specimen was observed when HA of 3000mg/cc was scanned at two different sizes with the same CT specifications. For the CBCT, the small HA (16mm³) was severely pixelated and the standard error was extremely large. When HA was large (467mm³), however, the standard error was much lower and more comparable to the standard error of measurements from the small and medium HA scanned with the micro XCT. The SA:V ratio for the small HA was 4 (16:4) whereas the SA:V ratio of the large HA was 1.02 (148:145). As the size of HA increases, the surface area to volume ratio decreases. When this ratio decreases, the SE of CBCT 1 system showed a much lower standard error compared to the small specimen.

Discussion

Based on the grayscale value measurements, there were distinct steps for each layer of the phantom scanned with the micro XCT. The grayscale values for the phantoms scanned with the CBCT machines were able to be somewhat differentiated on heat maps but the individual layers were not distinct. Values would rather be interpreted as a gradual change of density throughout the phantom. Overall grayscale values were significantly less in both CBCT machines compared to micro XCT machine due to the inferior resolution of these machines scanning at the field of view in which the image was captured. Calibration curves were created for each of the three CT machines based on gray value and known mineral density measurements of the phantom. All three curves had a positive slope as expected but the magnitude of the slope was much

lower in both CBCT machines relative to the micro XCT machine, which is known to be the gold standard in imaging. The same known mineral density produced a much lower grayscale reading in the CBCT machines, indicating possible problems with assessing true mineral density of specimens and/or pathology.

The amount of bleeding between layers was demonstrated by the phantom gray value distribution and plot profiles of mineral density. The phantom had a spatial resolution of 5 $\mu\text{m}/\text{pixel}$ and each mineral density layer had normally distributed values with clear peaks between layers. CBCT1 had a spatial resolution of 250 $\mu\text{m}/\text{pixel}$ and CBCT2 had a spatial resolution of 150 $\mu\text{m}/\text{pixel}$. Both of these were quite pixelated and displayed non-normal distribution without any clear peaks or distinctions between layers. The inferior level of resolution of the CBCT machines was clearly illustrated through these differing grayscale values and through the stark contrast in image quality of each phantom imaged with the different CT machines.

When the same type of segmentation and analysis was performed on mandibular incisors, differences in quality was further elucidated. Four different components (enamel, dentin, cortical bone, and trabecular bone) were analyzed. Graphical representations of the measurements for each of these revealed a normal distribution of mineral density for each component with the micro XCT scanner but a non-normal distribution for all CBCT measurements except for cortical bone. The pattern of these measurements and histograms were similar to those generated by the phantoms. The mineral density value of enamel, dentin, cortical bone, and trabecular bone varied in magnitude and range among all three scanning systems. CBCT1 severely underestimated the mineral density for each component. MD of enamel and trabecular

bone in CBCT 1 and 2 were the farthest off from MD as measured by micro XCT. Enamel is likely far off due to the size effect – the surface area to volume ratio is too small, there is lots of bleeding due to large pixel size, and the MD is unable to be measured accurately. Trabecular bone is likely far off due to the large marrow spaces and bleeding of pixels making it difficult to capture accurate density measurements. This likely happened with CBCT2 as well, but since the resolution is better given the smaller field of view, measurements were slightly more accurate. CBCT2 had mineral densities between micro XCT and CBCT1 but the range of measured values was often the greatest. This continues to illustrate the inconsistency and inaccuracy in CBCT mineral density measurements done under a large field of view with small specimens.

Enamel, dentin, cortical bone, and trabecular bone varied amongst all five individuals. The range of these differences was quite large. In the general population, enamel and dentin have a relatively consistent mineral density between individuals yet the measurements from the CBCT scans did not show much consistency. These values were also all much lower than the typical mineral density values of enamel (2820-3095 mg/cc), dentin (1480-1490mg/cc), and bone (570-1415 mg/cc) (Djomehri et al. 2015). The current imaging modality with the specifications used, even with the calibration curve, cannot accurately detect MD for enamel, dentin, and bone.

CBCT1 can detect apparent larger structural defects, existing fillings, and root canals especially when there is a stark difference in contrast between the defect or dental materials relative to the dental structures. It would be ideal to determine osseointegration and caries but this is not validated. It can possibly pinpoint areas of osseointegration and potential caries although given our findings this is unlikely to be

reliable. The poor resolution, large of amount of bleeding, the small size, and minimal differences in density make it very difficult to definitively diagnose either of these using a CBCT machine with the field of view similar to that of CBCT1 or CBCT 2.

It was determined that as the size of HA increases, the surface area to volume ratio decreases. For context, the SA:V ratio for the components of the teeth and jaws that we measured were all upwards of 1.02, thus indicating a large ratio and subsequently large standard of error. Enamel and trabecular bone have the largest ratio (~3) and those were the most inaccurate measurements whereas dentin and cortical bone were slightly more accurate as the SA:V ratio was about 1/2 to 1/3 of enamel and trabecular bone. This elucidates how the CBCT machine taken with a large field of view is too pixelated to definitely give consistent and accurate quantitative information about small structures within the maxillomandibular complex. If pathology or structures were large enough, the information that can be gleaned from them is more reliable. If suspected pathology is present, it is still advisable at this point to refer for more localized imaging with smaller field of view and better resolution to accurately pinpoint structural and pathological defects.

As the number of adult orthodontic patients has continued to increase and as patients who get dental implants tend to be more of the adult population, the ability to properly interpret CBCT scans could have profound consequences on treatment outcomes. As previously established in many studies, specific types of bone lead to better implant stability and overall success. Placement, number, and type of implant varies based on the properties of the bone in a specific region. With better knowledge of the density and structure of the bone in which the implant would be placed, greater

accuracy, success, and stability of implant placement can be achieved for optimal patient care. Baseline CBCTs are now often obtained for these older patients. If there was potential to screen every seemingly asymptomatic and “healthy” patient, it could be possible to potentially predict the development of significant future pathology such as bone diseases including osteopenia, osteoporosis, and/or medication related changes in mineral density of mineralized tissues including enamel and dentin (CBCT cannot resolve cementum).

It is well-established that bone mineral density in certain areas of the body can help predict occurrence of osteoporotic fracture but this has not been established within the jaws. Screening older individuals for baseline mineral density as obtained using CBCT scans, one could encourage earlier follow-up from their primary care physician to obtain more reliable bone mineral density tests that are already validated to determine risk of fracture and response to treatment. Eventually, it would be ideal to be able to correlate jaw bone density with hip or lumbar spine density. The earlier the risk assessment for bone pathology such as osteopenia or osteoporosis, the more likely an effective treatment rendering a successful outcome can be delivered to the patient. Screening to detect onsets of disease, requires a high resolution scanner to determine mineral density and/or structure and detect changes over time when multiple scans have been utilized.

There are several limitations of the current study. Regarding image capture of the specimens, dose rate and flux are not the same across XCT systems making the greyscale measurement and calibration process more difficult. The phantoms, which were used for calibration, only have a MD that goes up to 750 mg/cc. Most structures

within the maxilla and mandible have mineral densities greater than this number (i.e., enamel is >2000mg/cc) so the phantoms could have been fabricated differently for a more accurate reflection of the maxillomandibular complex. The CBCT images of the skull were taken from a pre-existing database and the movement of these individuals during capture could not be controlled for. Movement upon scan capture blurs images and sections making resolution poorer and blurrier. This is a problem in general when taking CBCT images, and it likely affects the analysis that was performed. Soft tissue effects were not taken into consideration during calibration process which may have affected the results. It was also difficult to ensure that the 2D slices were taken from the same area each time segmentation was performed, compromising potential accuracy as well. Bone density, in particular, is more likely to vary between individuals based on certain factors (i.e., age) whereas enamel and dentin tends to remain similar in structure and composition between healthy, non-diseased individuals. Specific factors and characteristics that could affect these measurements were not fully described or discussed.

Every instrument has its limitations, many of which have been described above for CBCT systems with a large field of view. These scans are currently being used as diagnostic unit and have many strengths when it comes to diagnosis and treatment planning. It would be ideal to use even more of the information on each scan for the patient's benefit but it still is only a binary system. It can only visualize the end stage scenario with specific parameters (i.e., mineral density magnitude and size dependence). When thinking in terms of screening for prevention of disease, this does not work well at the current moment in time and this needs to be questioned in terms of

limitations. It is unlikely to capture the inception of disease or capture/diagnose on a routinely captured CBCT scan from a dentist or specialist with a field of view 8 x 9 or larger. It is likely that a lesion or pathology can only be diagnosed reliably when it is a large enough density and size for us to actually utilize or if it imaged under a smaller field of view with enhanced resolution. As the quality of CT scanning systems increase and enhanced calibration efforts are undertaken, it will be within the realm of possibility to not only use routine imaging of orthodontic patients as a diagnostic tool but also as a screening tool to potentially prevent future disease from occurring.

References

- Algerban, A., Jacobs, R., Souza, P. C., & Willems, G. (2009). In-vitro comparison of 2 cone-beam computed tomography systems and panoramic imaging for detecting simulated canine impaction-induced external root resorption in maxillary lateral incisors. *American Journal of Orthodontics and Dentofacial Orthopedics*, 136(6), 764-e1.
- Angelopoulos, C., Thomas, S., Hechler, S., Parissis, N., & Hlavacek, M. (2008). Comparison between digital panoramic radiography and cone-beam computed tomography for the identification of the mandibular canal as part of presurgical dental implant assessment. *Journal of Oral and Maxillofacial Surgery*, 66(10), 2130-2135.
- Aranyarachkul, P., Caruso, J., Gantes, B., Schulz, E., Riggs, M., Dus, I., Yamada, J.M. & Crigger, M. (2005) Bone density assessments of dental implant sites: 2. Quantitative cone-beam computerized tomography. *The International Journal of Oral & Maxillofacial Implants* 20: 416–424.
- Bouwens, D. G., Cevdanes, L., Ludlow, J. B., & Phillips, C. (2011). Comparison of mesiodistal root angulation with posttreatment panoramic radiographs and cone-beam computed tomography. *American journal of orthodontics and dentofacial orthopedics*, 139(1), 126-132.
- Cassetta, M., Stefanelli, L.V., Pacifici, A., Pacifici, L. & Barbato, E. (2013) How accurate is CBCT in measuring bone density? A comparative CBCT-CT in vitro study. *Clinical Implant Dentistry and Related Research*. doi: 10.1111/cid. 12027.
- Chugh, T., Jain, A. K., Jaiswal, R. K., Mehrotra, P., & Mehrotra, R. (2013). Bone density

and its importance in orthodontics. *Journal of oral biology and craniofacial research*, 3(2), 92-97.

DenOtter TD, Schubert J. Hounsfield Unit. [Updated 2019 Oct 6]. In: StatPearls [Internet]. Treasure Island (FL): StatPearls Publishing; 2020 Jan-.

Djomehri, S. I., Candell, S., Case, T., Browning, A., Marshall, G. W., Yun, W., ... & Ho, S. P. (2015). Mineral density volume gradients in normal and diseased human tissues. *PLoS One*, 10(4).

Ghaeminia, H., Meijer, G. J., Soehardi, A., Borstlap, W. A., Mulder, J., & Bergé, S. J. (2009). Position of the impacted third molar in relation to the mandibular canal. Diagnostic accuracy of cone beam computed tomography compared with panoramic radiography. *International journal of oral and maxillofacial surgery*, 38(9), 964-971.

Ghaeminia, H., Meijer, G. J., Soehardi, A., Borstlap, W. A., Mulder, J., Vlijmen, O. J. C., ... & Maal, T. J. J. (2011). The use of cone beam CT for the removal of wisdom teeth changes the surgical approach compared with panoramic radiography: a pilot study. *International journal of oral and maxillofacial surgery*, 40(8), 834-839.

Honey, O. B., Scarfe, W. C., Hilgers, M. J., Klueber, K., Silveira, A. M., Haskell, B. S., & Farman, A. G. (2007). Accuracy of cone-beam computed tomography imaging of the temporomandibular joint: comparisons with panoramic radiology and linear tomography. *American journal of orthodontics and dentofacial orthopedics*, 132(4), 429-438.

Jadu, F. M., & Lam, E. W. N. (2013). A comparative study of the diagnostic capabilities

- of 2D plain radiograph and 3D cone beam CT sialography. *Dentomaxillofacial Radiology*, 42(1), 20110319-20110319.
- Kravitz N.D., Kusnoto B., Tsay T.P., Hohit W.F. The use of temporary anchorage devices for molar intrusion. *J Am Dent Assoc.* 2007;138(1):56–64.
- Lekholm U., Zarb G.A. Patient selection and preparation. In: Brånemark P.-I., Zarb G.A., Albrektsson T., editors. *Tissue-integrated Prostheses: Osseointegration in Clinical Dentistry*. Quintessence; Chicago: 1985. pp. 199–209
- Ludlow, J. 2014. Dosimetry of CS 9300 Low-Dose Protocol. University of North Carolina, School of Dentistry.
- Mah P, Reeves TE, McDavid WD. (2010). Deriving Hounsfield units using grey levels in cone beam computed tomography. *Dentomaxillofac Radiol.* 2010 Sep; 39(6):323-35.
- Misch C.E., Kircos L.T. Diagnostic imaging and techniques. In: Misch C.E., editor. *Contemporary Implant Dentistry*. 2nd ed. Mosby; St. Louis: 1999. pp. 73–87.
- Misch C.E. (1990). Density of bone: effect on treatment plans, surgical approach, and healing, and progressive loading. *Int J Oral Implantol.*; 6:23–31.
- Naitoh, M., Hirukawa, A., Katsumata, A. & Arijii, E. (2009) Evaluation of voxel values in mandibular cancellous bone: relationship between cone-beam computed tomography and multislice helical computed tomography. *Clinical Oral Implants Research* 20: 503–506.
- Parsa A, Ibrahim N, Hassan B, Motroni A, van der Stelt P, Wismeijer D. (2012). *Int J Oral Maxillofac Implants.* Nov-Dec; 27(6):1438-42. Reliability of voxel gray

values in cone beam computed tomography for preoperative implant planning assessment.

Parsa, A., Ibrahim, N., Hassan, B., van der Stelt, P., & Wismeijer, D. (2015). Bone quality evaluation at dental implant site using multislice CT, micro-CT, and cone beam CT. *Clinical oral implants research*, 26(1), e1-e7.

Razi, T., Niknami, M., & Ghazani, F. A. (2014). Relationship between Hounsfield unit in CT scan and gray scale in CBCT. *Journal of dental research, dental clinics, dental prospects*, 8(2), 107.

Reeves, T., Mah, P. & McDavid, W.D. (2012) Deriving Hounsfield units using grey levels in cone beam CT: a clinical application. *Dentomaxillofacial Radiology* 41: 500–508.

Truhlar, R. S., Orenstein, I. H., Morris, H. F., & Ochi, S. (1997). Distribution of bone quality in patients receiving endosseous dental implants. *Journal of Oral and Maxillofacial Surgery*, 55(12), 38-45.

Voumard, B., Maquer, G., Heuberger, P., Zysset, P. K., & Wolfram, U. (2019). Peroperative estimation of bone quality and primary dental implant stability. *Journal of the mechanical behavior of biomedical materials*, 92, 24-32.

Publishing Agreement

It is the policy of the University to encourage open access and broad distribution of all theses, dissertations, and manuscripts. The Graduate Division will facilitate the distribution of UCSF theses, dissertations, and manuscripts to the UCSF Library for open access and distribution. UCSF will make such theses, dissertations, and manuscripts accessible to the public and will take reasonable steps to preserve these works in perpetuity.

I hereby grant the non-exclusive, perpetual right to The Regents of the University of California to reproduce, publicly display, distribute, preserve, and publish copies of my thesis, dissertation, or manuscript in any form or media, now existing or later derived, including access online for teaching, research, and public service purposes.

DocuSigned by:

Yianni Ellenikiotis

FBC40518F75B462...

Author Signature

6/6/2020

Date